DBMC-NOMA: Evaluating NOMA for Diffusion-Based Molecular Communication Networks

Alexander Wietfeld, Sebastian Schmidt, Wolfgang Kellerer

Chair of Communication Networks
Technical University of Munich
Munich, Germany
{alexander.wietfeld, sebastian.a.schmidt, wolfgang.kellerer}@tum.de

Abstract—This paper presents an evaluation of non-orthogonal multiple access (NOMA) as a novel approach for diffusion-based molecular communication (DBMC) networks. The scheme draws from the example of power-domain NOMA in classical communication and relies on differences in the number of received molecules. It utilizes successive interference cancellation to separate simultaneously transmitted messages from multiple transmitters (TXs) at the receiver (RX) using a single molecule type. We analytically derive the bit error probability of a communication system using DBMC-NOMA with K TXs and a central RX and validate the model with Monte Carlo simulations. Our results show that the emitted number of molecules from each TX is a crucial parameter to optimize the performance of DBMC-NOMA. Additionally, we compare the performance of DBMC-NOMA against time-division multiple access (TDMA) and molecule-division multiple access (MDMA) with respect to the mutual information at the RX. The investigation shows that TDMA and MDMA act as the lower and upper performance bounds for DBMC-NOMA, respectively. For a sufficiently large molecule budget and SNR, DBMC-NOMA outperforms TDMA and matches MDMA using only one molecule type even as the number of TXs grows. These results show the potential of NOMA as an option for DBMC and the need for further analysis of power control schemes to optimize the number of emitted molecules in DBMC networks.

Index Terms—molecular communication, non-orthogonal multiple access, NOMA, bit error probability

I. INTRODUCTION

Diffusion-based molecular communication (DBMC) is a communication method based on the transfer of molecules as information carriers. It has garnered increasing attention in recent years due to shortcomings of classical electromagnetic communication in scenarios with strict requirements on the size and energy efficiency of the nodes, as well as for applications with bio-compatibility concerns. Some of the main motivations behind DBMC are expected use cases for in-body networks as part of an Internet of Bio-Nano-Things (IoBNT) [1]. For example, in future bio-medical applications, DBMC is expected to enable connections between small bio-nano-machines (BNMs) with limited capability to perform different tasks such as absorption and emission of, or reaction to, molecules in the environment. To enable more complex tasks like targeted drug delivery or identification of infections

and tumors [1], multiple transmitter (TX) BNMs might need to communicate simultaneously with one receiver (RX) BNM. For the RX to differentiate between data sources, such as the different types of BNMs or locations in the body, multiple access (MA) is necessary.

Different MA schemes have been proposed and investigated for DBMC, such as time-division multiple access (TDMA) [2] or molecule-division multiple access (MDMA) [3]. TDMA assigns a different time slot to each TX so that their transmissions do not interfere. For MDMA, a different molecule type is used by each TX, which the RX can separate on reception. TDMA enables single-molecule-type MA, lowering the requirements towards the physical complexity of the nodes since, for example, the RX only needs one type of molecule receptor. In contrast, MDMA enables simultaneous transmissions from all TXs, which facilitates higher system throughput but at the cost of higher physical complexity. However, both single-molecule-type MA and simultaneous transmissions are desirable for achieving a low-complexity, high-capacity DBMC network.

Non-orthogonal multiple access (NOMA) has been explored extensively for classical electromagnetic-wave-based (EM) communication networks as a means to increase network capacity without requiring more frequency channels. In its most common form of power-domain NOMA, it utilizes the level of transmission power to differentiate TXs within the same frequency band [4]. Comparing EM and DBMC, we can draw parallels between orthogonal frequency bands and molecule types, as well as the transmission power and the emitted number of molecules. Following this analogy, NOMA could enable MA in DBMC networks without increasing the required number of molecule types.

Using amplitude to differentiate TXs was first proposed for a bacterial communication system in [5], where the received number of molecules is utilized as a source address. The authors design a set of amplitudes such that the sum of any subset can be used to unambiguously identify the sources of the messages, and assume a constant bit error probability (BEP). The decoder is designed to choose the most likely combination of TXs based on a deterministic codebook of received amplitudes. In contrast, NOMA uses successive interference cancellation (SIC) to extract the transmitted symbols based on channel estimation and signal processing.

In [6], we first proposed the investigation of NOMA for DBMC networks (DBMC-NOMA) based on the number of received molecules at the RX to provide single-molecule-type MA with simultaneous transmissions. We presented a simplified model with preliminary results, which showed promise in the further analysis and optimization of DBMC-NOMA. In this paper, we extend our previous work [6] in several key areas:

1) We derive an analytical model for the BEP of DBMC-NOMA in a network with K TXs considering inter-symbol interference (ISI) up to L time slots and verify the model via Monte Carlo simulations (MCSs).

2) We investigate the influence of the optimal choice of detection thresholds and the emitted number of molecules per TX on the BEP of DBMC-NOMA.

3) Using the analytical model, we compare TDMA, MDMA, and DBMC-NOMA with respect to the achievable mutual information at the RX for varying network sizes and additive noise levels. We show that DBMC-NOMA generally outperforms TDMA and achieves the same performance as MDMA for a sufficiently large molecule budget per TX and signaling-molecule-to-noise ratio (SNR).

II. SYSTEM MODEL

Figure 1 depicts a simple communication network schematic modeling the IoBNT use case described in Section I. The network consists of K TXs TX$_1$, …, TX$_K$ at distances $d_1 \leq d_2 \leq \cdots \leq d_K$ from a single spherical RX with radius r. The TXs are modeled as point sources, which can instantaneously emit pulses of molecules into the surrounding unbounded three-dimensional space. The emitted molecules are affected by Brownian motion with diffusion coefficient D. The RX is assumed to be passive and the received signal is the number of molecules within the RX volume over time.

Firstly, we will look at an individual channel between TX$_i$ and the RX at a distance d_i. If TX$_i$ emits a single molecule at time $t = 0$, the probability of observing it at time t within the RX volume of size V_{RX} is derived in [7] as

$$P_i(t) = P(t, d_i) = \frac{V_{\text{RX}}}{(4\pi D t)^{\frac{3}{2}}} \exp\left(-\frac{d_i^2}{4Dt}\right). \quad (1)$$

Eq. (1) presupposes the so-called uniform concentration assumption (UCA), which is valid for $r < 0.15 d_i$ [7]. We assume independent molecule behavior, that the number of molecules $N_{\text{TX},i}$ emitted from TX$_i$ is large, and that only a small fraction of molecules arrive at the receiver. In this case, the received signal $n_{\text{RX}}(t)$ is commonly modeled as a Poisson-distributed random variable with mean $\lambda_i(t) = N_{\text{TX},i} P_i(t)$ such that $n_{\text{RX}}(t) \sim \mathcal{P}(\lambda_i(t))$ [7].

A. Communication System Assumptions

To transmit information, the TXs utilize on-off-keying, where a '1' is represented by a pulse of $N_{\text{TX},i}$ molecules. Symbols '0' and '1' are assumed to be equally likely. Time is split into slots of length T, and the current time slot is
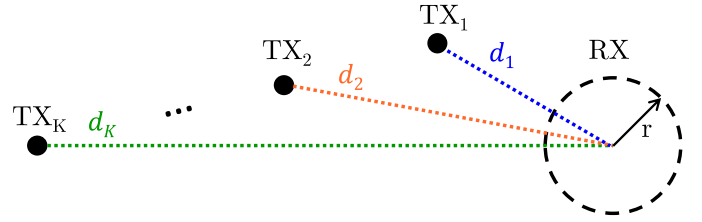

Fig. 1. DBMC scenario with K point transmitters at distances d_1, d_2 … d_K from a spherical receiver.

denoted as $l = 0$. The preceding L time slots in the past are $l \in \{1, 2, \ldots, L\}$. Time is measured relative to the beginning of slot $l = 0$, starting at $t = 0$ and ending at $t = T$. The symbol sent by TX$_i$ in time slot l is denoted by $s_i[l]$. We assume the network is perfectly synchronized, and the TXs send a pulse of $s_i[l] N_{\text{TX},i}$ molecules at the beginning of a time slot. Additionally, we assume accurate channel and distance information at the RX. For decoding, the RX can therefore take a sample of the received signal at the expected peak time of the molecules arriving from the TX it is currently decoding.

To differentiate the TX currently targeted for decoding from the influences on the received signal by other TXs, we denote the former and the corresponding peak time with the index j as TX$_j$ and $t_{\text{p},j}$, and continue to denote the latter as TX$_i$. The peak time for the signal from TX$_j$ can be derived from (1) as $t_{\text{p},j} = \frac{d_j^2}{6D}$. We now define the average of the signal component from TX$_i$, sampled at the expected peak time of TX$_j$, for a transmitted '1' in time slot l as

$$\lambda_{i,j}[l] = \lambda_i\left(t_{\text{p},j} + lT\right). \quad (2)$$

Additionally, we denote the $\lambda_{i,j}[l]$ at the corresponding peak for each TX$_i$ as

$$\tilde{\lambda}_i = \lambda_{i,i}[0] = \lambda_i\left(t_{\text{p},i}\right). \quad (3)$$

The overall received signal at the sampling points $n_{\text{RX}}(t_{\text{p},j})$ is a sum of multiple independent Poisson variables, each with a mean according to (2). The sum of multiple independent Poisson variables is also a Poisson variable and its mean is the sum of the means of the added variables. Detection of molecules due to unintended leakages from molecule reservoirs or interference from unrelated biochemical processes can additionally increase the number of received molecules. We assume additive Poisson noise with mean λ_{n} to represent these environmental noise factors.

To detect the symbol sent by TX$_j$, the RX employs threshold $\tau_j \geq 0$ with the decision rule

$$\hat{s}_j = \begin{cases} 1 & n_{\text{sample},j} \geq \tau_j \\ 0 & n_{\text{sample},j} < \tau_j \end{cases}, \quad (4)$$

where $n_{\text{sample},j}$ is the value used by the RX to conduct the detection and $\hat{s}_j$ is the detected symbol.

B. Multiple Access Schemes

Based on the information available at the TXs and RX, the MA scheme decides which TX$_i$ is assigned to transmit

in time slot l and how the signals are differentiated at the RX. The arriving signals must be manipulated in some way to be distinct. For this purpose, TDMA, MDMA, and DBMC-NOMA use different dimensions of manipulation, which are time, molecule type, and received signal level, respectively. The choice of dimension results in different rules for the transmission and reception process.

1) MDMA: Since the TXs each use one of K different molecule types perfectly distinguishable at the RX, there is no multiple-access interference (MAI) between the TXs. We also assume that all molecule types share the same diffusion coefficient. Each TX_j is assigned every time slot to transmit symbols. The communication can be modeled through K independent received signals. Considering only the molecule type used by TX_j, the received signal at $t_{p,j}$ is

$$n_{\mathrm{RX},j}^{\mathrm{MDMA}}(t_{p,j}) \sim \mathcal{P}\left(\lambda_n + s_j[0]\tilde{\lambda}_j + \underbrace{\sum_{l=1}^{L} s_j[l]\lambda_{j,j}[l]}_{\mathrm{ISI}}\right), \quad (5)$$

which contains the component sent by TX_j in the current time slot $s_j[0]\tilde{\lambda}_j$ and ISI from the transmissions in the previous L time slots. We assume that the RX has access to the K different received signals, i.e. for the detection of the symbol from TX_j in the current slot, we have $n_{\mathrm{sample},j} = n_{\mathrm{RX},j}^{\mathrm{MDMA}}(t_{p,j})$.

2) TDMA: Each time slot is assigned to a single TX. If the current time slot is assigned to TX_j, then the previous time slots were assigned to the other TXs in descending order of the indices until looping around from 1 to K. We assume the RX knows which TX_j transmits in the current time slot, and therefore it performs threshold detection on the received signal at $t_{p,j}$. The received signal $n_{\mathrm{RX}}^{\mathrm{TDMA}}(t_{p,j})$ contains the component from TX_j sent in the current time slot and ISI from all the TXs in the previous L slots. Since its structure is essentially identical to (5), except the ISI is caused by transmissions from the TXs assigned to the previous L time slots and not just by TX_j, it is omitted for brevity.

3) NOMA: Similar to MDMA, all K TXs are assigned to every time slot. Since they use the same molecule type, the received signal includes overlapping components from different TXs. The received signal at $t_{p,j}$, can be written as

$$n_{\mathrm{RX}}^{\mathrm{NOMA}}(t_{p,j}) \sim \mathcal{P}\left(\lambda_n + \sum_{i=1}^{K}\sum_{l=0}^{L} s_i[l]\lambda_{i,j}[l]\right)$$
$$= \mathcal{P}\left(\lambda_n + s_j[0]\tilde{\lambda}_j + \underbrace{\sum_{\substack{i=1 \\ i\neq j}}^{K} s_i[0]\lambda_{i,j}[0]}_{\mathrm{MAI}} + \underbrace{\sum_{i=1}^{K}\sum_{l=1}^{L} s_i[l]\lambda_{i,j}[l]}_{\mathrm{ISI}}\right). \quad (6)$$

In addition to ISI, the signal contains MAI from other symbols transmitted in the same time slot. A SIC technique, similar to the one proposed for NOMA in [4], is used to remove the MAI and thereby separate the signals at the RX. The detection within the current time slot takes place iteratively, starting from the TX with the highest $\tilde{\lambda}_i$. We assume the TX indices reflect the descending order with respect to $\tilde{\lambda}_i$.

Therefore, the detection starts with TX_1. In the first step, $\hat{s}_1$ is obtained using (4) with $n_{\mathrm{sample},1} = n_{\mathrm{RX}}^{\mathrm{NOMA}}(t_{p,1})$. In the second step, the RX uses its knowledge of the channel to subtract $\hat{s}_1\lambda_{1,2}[0]$, the expected component of TX_1 at the sampling time for TX_2, from the received signal. The resulting sample, $n_{\mathrm{sample},2} = n_{\mathrm{RX}}(t_{p,2}) - \hat{s}_1\lambda_{1,2}[0]$ is used for obtaining $\hat{s}_2$. Continuing this procedure for all TXs, we can write the signal after SIC for detection of the symbol from TX_j as

$$n_{\mathrm{sample},j} = n_{\mathrm{RX}}(t_{p,j}) - \sum_{i=1}^{j-1} \hat{s}_i\lambda_{i,j}[0]. \quad (7)$$

While this formula can lead to values of the sample with $n_{\mathrm{sample},j} < 0$, we note that in a real DBMC system the number of molecules used for a sample can not be below zero. This has no effect on the results however, since $\tau_j \geq 0$ holds for the detection. Therefore, sample values below zero are treated as if they were equal to zero.

III. ANALYTICAL BIT ERROR PROBABILITY DERIVATION

Firstly, we denote the BEP of the individual TX_i as $P_{\mathrm{e},i}$. Additionally, we consider the system BEP $P_{\mathrm{e,sys}}$ as the probability that any transmitted symbol in a given time slot is erroneously detected:

$$P_{\mathrm{e,sys}} = \frac{1}{K}\sum_{i=1}^{K} P_{\mathrm{e},i}. \quad (8)$$

In the following, we present the derivation of the BEP for a network of K TXs according to Figure 1 using DBMC-NOMA. To start, we introduce auxiliary variables based on the definitions from Section II. Firstly, we write the vector of all expected signal values for a sample at $t_{p,j}$, for transmission from all TXs in time slots from $l = 0$ to L as

$$\mathbf{\Lambda}_j = [\lambda_{1,j}[0], \cdots, \lambda_{K,j}[0], \lambda_{1,j}[1], \cdots, \lambda_{K,j}[1],$$
$$\cdots, \lambda_{1,j}[L], \cdots, \lambda_{K,j}[L]]. \quad (9)$$

Secondly, we define the set of all vectors of length N with binary elements as $\mathbb{B}^N = \{[b_0 b_1 b_2 \cdots b_N] \mid b_i \in \{0,1\}\}$. Based on this, we write the vector of all transmitted symbols in all time slots from $l = 0$ to L as

$$\mathbf{S} = [s_1[0], \cdots, s_K[0], s_1[1], \cdots, s_K[1],$$
$$\cdots, s_1[L], \cdots, s_K[L]] \in \mathbb{B}^{K(L+1)}, \quad (10)$$

such that $\mathbf{S} \cdot \mathbf{\Lambda}_j = \sum_{i=1}^{K}\sum_{l=0}^{L} s_i[l]\lambda_{i,j}[l]$ as in (6). Similarly, we define a vector of all the decoded symbols in the current time slots for the TXs up to and including TX_m

$$\underline{\hat{s}}_m = [\hat{s}_1, \hat{s}_2, \cdots, \hat{s}_m] \in \mathbb{B}^m. \quad (11)$$

We will now consider the case of decoding the symbol from TX_j in the current time slot after having decoded the symbols of TX_1 to TX_{j-1}. We define the probability of the sample for TX_j after SIC being below the threshold τ_j given that

$s_j[0] = x \in \{0,1\}$ as $P_{j,x} = \mathbb{P}\left(n_{\text{sample},j} < \tau_j | s_j[0] = x\right)$. Based on (7), we can manipulate $n_{\text{sample},j} < \tau_j$, such that

$$P_{j,x} = \mathbb{P}\left(n_{\text{RX}}(t_{\text{p},j}) < \tau_j + \sum_{i=1}^{j-1} \hat{s}_i \lambda_{i,j}[0] | s_j[0] = x\right). \quad (12)$$

Using (12) and $\mathcal{P}_{\text{CDF}}(m; \lambda) = \sum_{k=0}^{m} \lambda^k \frac{e^{-\lambda}}{k!}$, which denotes the evaluation of the cumulative density function of the Poisson distribution at m, we can calculate the conditional probability associated with $P_{j,x}$ when all transmitted symbols $\mathbf{S}$ and the previously decoded symbols $\hat{\underline{s}}_{j-1}$ are given, as

$$\mathbb{P}\left(n_{\text{sample},j} < \tau_j \mid s_j[0] = x, \mathbf{S} = \mathbf{S}', \hat{\underline{s}}_{j-1} = \hat{\underline{s}}'_{j-1}\right)$$
$$= \mathcal{P}_{\text{CDF}}\left(\tau_j - 1 + \sum_{i=1}^{j-1} \hat{s}'_i \lambda_{i,j}[0]; \mathbf{S}' \cdot \mathbf{\Lambda}_j + \lambda_n\right). \quad (13)$$

To arrive at the marginal probability, we must form the sum over all possible cases for $\mathbf{S}$ (with $s_j[0] = x$) and $\hat{\underline{s}}_{j-1}$ multiplied by the respective probability of occurrence for each case. Since there are symbols across $L+1$ time slots from K different transmitters considered in the received signal, there are $2^{K(L+1)}$ different equiprobable combinations of transmitted symbols $\mathbf{S}$, which affect the mean of the received signal's Poisson distribution. Additionally, 2^{j-1} different possible combinations of detected symbols $\hat{\underline{s}}_j$ for the previously considered TXs in the current time slot affect the SIC applied to the received signal up to TX_j. The probability of each $\hat{\underline{s}}_j$ occurring depends on $\mathbf{S}$ and on the BEPs for the previously considered TXs. We note that therefore, $\mathbb{P}\left(\mathbf{S} = \mathbf{S}' \in \mathbb{B}^{K(L+1)} \mid s_j[0] = x\right) = \frac{1}{2^{(K(L+1)-1)}}$ and refer to the Appendix for the calculation of $\mathbb{P}\left(\hat{\underline{s}}_{j-1} = \hat{\underline{s}}'_{j-1} \mid \mathbf{S} = \mathbf{S}', s_j[0] = x\right)$. Combining the latter with (12) and (13), we get

$$P_{j,x} = \sum_{\substack{\mathbf{S}' \in \mathbb{B}^{K(L+1)} \\ s_j[0]=x}} \sum_{\hat{\underline{s}}'_{j-1} \in \mathbb{B}^{j-1}} \mathbb{P}\left(\hat{\underline{s}}_{j-1} = \hat{\underline{s}}'_{j-1} | \mathbf{S} = \mathbf{S}', s_j[0] = x\right)$$
$$\cdot \frac{1}{2^{(K(L+1)-1)}} \mathcal{P}_{\text{CDF}}\left(\tau_j - 1 + \sum_{i=1}^{j-1} \hat{s}'_i \lambda_{i,j}[0]; \mathbf{S}' \cdot \mathbf{\Lambda}_j + \lambda_n\right). \quad (14)$$

We note that $P_{j,x}$ corresponds to the probability of correct detection if $x = 0$, and to the probability of incorrect detection if $x = 1$. Therefore, the BEP of TX_j is given by

$$P_{e,j} = \frac{1}{2}\left(P_{j,1} + (1 - P_{j,0})\right). \quad (15)$$

Similar derivations exist for TDMA [8], and MDMA, for which we consider K independent communication links [9].

IV. EVALUATION

Results of the evaluation of the BEP model above will be presented in the following. Table I lists the simulation parameters. Underlined values are always used unless otherwise stated. The parameters are chosen such that the UCA can be applied and the Poisson distribution can be used, as introduced in Section II.

Parameter	Symbol	Value (Default)
Number of TXs	K	$\{\underline{2}, 3, 4, 5\}$
TX distances	$\{d_1, d_2, \ldots, d_K\}$	$10\,\mu\text{m}$
RX radius	r	$1\,\mu\text{m}$
Symbol period	T	$1\,\text{s}$
ISI length	L	1
Diffusion coefficient	D	$10^{-9}\,\text{m}^2\,\text{s}^{-1}$
Signaling-molecule-to-noise ratio	SNR	$10^{-2} \leq \text{SNR} \leq \infty$

For comparison of the different MA schemes, the mutual information per time slot at the RX is considered. The mutual information due to a transmission from TX_i in the current time slot can be obtained from the probability distributions of transmitted and received symbols, as described in [10], and is denoted as $\mathcal{I}_i$. For MDMA and NOMA, all TXs transmit in every time slot. In contrast, the mutual information for TDMA must be averaged across the K TXs since only one TX transmits per time slot. Therefore, the total mutual information per time slot at the RX, $\mathcal{I}_{\text{sys}}$, for MDMA and NOMA is $\mathcal{I}_{\text{sys}}^{\text{MDMA}} = \sum_{i=1}^{K} \mathcal{I}_i^{\text{MDMA}}$ and $\mathcal{I}_{\text{sys}}^{\text{NOMA}} = \sum_{i=1}^{K} \mathcal{I}_i^{\text{NOMA}}$, respectively, while for TDMA it is $\mathcal{I}_{\text{sys}}^{\text{TDMA}} = \frac{1}{K} \sum_{i=1}^{K} \mathcal{I}_i^{\text{TDMA}}$. Note, that we assume independent information sources for the messages sent by each TX such that we can sum the mutual information at the RX.

We define the SNR at the RX as the ratio of the highest $\tilde{\lambda}_i$ and the mean of the additive noise λ_n

$$\text{SNR} = \frac{\max_i \tilde{\lambda}_i}{\lambda_n}. \quad (16)$$

The SNR is utilized as an expression of the relative noise level in the following evaluation and does not represent a performance metric.

A. Analysis of DBMC-NOMA

The following results are focused on the analysis of DBMC-NOMA in isolation to highlight the effect of selected parameters on the performance.

1) Varying the Detection Threshold: Figure 2 depicts the value of $P_{e,i}$ over the respective τ_i for a network with $K = 2$ equidistant TXs. The TXs differ only in the number of emitted molecules with $N_{\text{TX},1} = 10^6$ and $N_{\text{TX},2} = 0.54 \cdot 10^6$. MCS additionally conducted based on the Poisson distributions of the received signal components with 10^6 randomly generated symbol vectors are shown along with the analytical results to validate the derivation.

Like the iterative detection process for DBMC-NOMA described in Section II-B, optimization of the τ_i is conducted iteratively. Since the detection process of TX_1 does not depend on prior detection steps, τ_1 can be chosen independently from τ_2, and a single optimum can be found. The detection for TX_2 depends on the choice of τ_1 and the resulting $P_{e,1}$. If we choose $\tau_1 = \tau_1^*$, there is a fixed $P_{e,1}$, and we can find a single optimum value τ_2^*. In Figure 2, $P_{e,2}$ is plotted under the assumption that $\tau_1 = \tau_1^* = 231$ such that $\tau_2^* = 78$ can
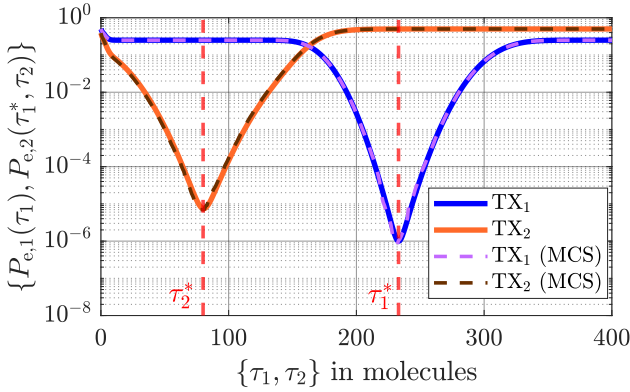
Fig. 2. Analytical bit error probabilities $P_{e,i}$ over the detection thresholds τ_i for a DBMC-NOMA system with $K = 2$ TXs. The plot shows $P_{e,1}(\tau_1)$ and $P_{e,2}(\tau_1^*, \tau_2)$, where we have set $\tau_1 = \tau_1^*$ to the optimal value. Numbers of emitted molecules are $N_{TX,1} = 10^6$ and $N_{TX,2} = 0.54 \cdot 10^6$. All other parameters chosen according to Table I. Monte-Carlo results are also shown.
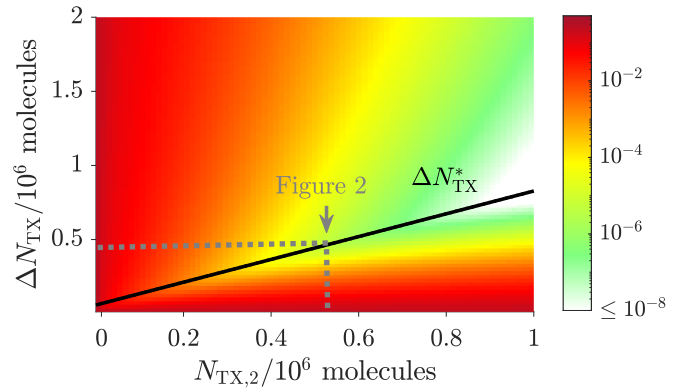

Fig. 3. Bit error probability $P_{e,sys}$ of a DBMC-NOMA system with $K = 2$ TXs for varying values of the emitted number of molecules $N_{TX,i}$. $\Delta N_{TX} = N_{TX,1} - N_{TX,2}$ is varied on the y-axis and $N_{TX,2}$ on the x-axis. Detection thresholds τ_i are chosen optimally. Optimum ΔN_{TX}^*, which minimizes $P_{e,sys}$ for a given $N_{TX,2}$, and the parameters used for Figure 2 are highlighted. All other parameters chosen according to Table I.

be identified. This procedure could be continued similarly for networks of size $K > 2$.

2) Varying the Number of Emitted Molecules: In Figure 3, $P_{e,sys}$ of a network with $K = 2$ applying optimum thresholds is shown on a heatmap as a function of the emitted numbers of molecules from each TX. $N_{TX,2}$ is varied on the x-axis, and $\Delta N_{TX} = N_{TX,1} - N_{TX,2}$ is varied on the y-axis such that $N_{TX,1} \geq N_{TX,2}$. Several effects are visible from the resulting pattern.

Firstly, for a given $N_{TX,2}$, it is possible to find an optimal value ΔN_{TX}^*. Suppose ΔN_{TX} is decreased from the optimum. In this case, the separation between the received signal values for the TXs becomes smaller, and it becomes harder to differentiate the signals by choosing an appropriate threshold in the first detection step for TX_1. Additionally, if $P_{e,1}$ increases, the SIC is more likely to apply the wrong correction to the sampled signal for TX_2, which increases $P_{e,2}$ as well. For a Poisson distribution, the variance of a signal sample is equal to the associated mean λ; therefore, the standard deviation is $\sigma = \sqrt{\lambda}$. If ΔN_{TX} increases, the signal from TX_1 grows larger compared to the signal from TX_2. After SIC, the standard deviation of the component from TX_1 remains as part of the signal since only the mean can be removed by the SIC. The deviation of the sample relative to the mean of the component from TX_2 increases, diminishing the detection performance for TX_2 and therefore $P_{e,sys}$.

The plot shows that $\Delta N_{TX}^* \propto N_{TX,2}$ holds for the chosen parameter range. Additionally, as $N_{TX,2}$ increases, we observe that ΔN_{TX}^* achieves a lower optimum $P_{e,sys}$. This effect can again be explained by the signal-dependent standard deviation σ of the DBMC signal. As λ increases, the standard deviation relative to the mean decreases since $\frac{\sigma}{\lambda} = \frac{1}{\sqrt{\lambda}}$. For higher values of $N_{TX,2}$ and ΔN_{TX}, the samples have a lower relative deviation from the mean. They are therefore more likely to be detected correctly.

B. Comparison of MA Schemes

The performance comparison between the MA schemes is based on the following assumptions. We consider a scenario with K TXs such that $d_1 = \cdots = d_K$. Each TX has a molecule budget $N_{TX,max}$, which sets an upper limit to the number of molecules $N_{TX,i}$ it can transmit per symbol period. The detection threshold is chosen through an exhaustive search, such that $\tau_i = \tau_i^*$ for all TXs. For TDMA and MDMA, we assume that $N_{TX,i} = N_{TX,max}$ for all TXs. For DBMC-NOMA, we assume that the detection at the RX is performed in ascending order of the TX index i. The maximum emitted number of molecules is always assigned to TX_1, i.e. $N_{TX,1} = N_{TX,max}$, while $N_{TX,2}, \ldots, N_{TX,K}$ are optimized via exhaustive search. To evaluate the effects of the varied parameters on the performance in isolation, we set the ISI length $L = 0$ and $SNR = \infty$, unless otherwise stated.

We note that in the context of the comparisons, MDMA represents the upper bound for the MA performance since it makes use of multiple molecule types to facilitate an independent communication channel for each TX.

1) Varying Noise Level: Figure 4 depicts $\mathcal{I}_{sys}$ per time slot over the SNR as defined by (16). We can observe that the performance curves of TDMA and MDMA serve as the lower and upper bounds for DBMC-NOMA, respectively. We first focus on the case of $N_{TX,max} = 10^6$. The graph shows that $\mathcal{I}_{sys}^{NOMA} \approx \mathcal{I}_{sys}^{MDMA}$ for $SNR > 1$ and $\mathcal{I}_{sys}^{NOMA} \approx \mathcal{I}_{sys}^{TDMA}$ for $SNR < 0.1$. The transition in between is caused primarily by a decrease in the performance of TX_2. In the low SNR regime, DBMC-NOMA essentially serves only one TX at twice the rate that TDMA serves each of the two TX. This is caused by the optimization goal targeting the overall system performance. An additional analysis of the fairness resulting from the different MA schemes with respect to the performance of individual TXs using, for example, the min-max BEP metric is left for further work.
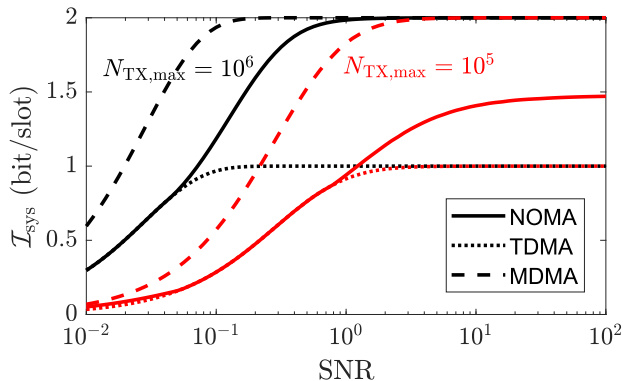
Fig. 4. Mutual information per time slot $\mathcal{I}_\text{sys}$ over the SNR for three different MA schemes. Detection thresholds τ_i and number of emitted molecules $N_{\text{TX},i}$ are chosen optimally subject to different maximum molecule budgets $N_{\text{TX,max}}$ per TX per time slot. For all other parameters see Table I. In the low-SNR regime NOMA performs similarly to TDMA, and in the high-SNR regime similarly to MDMA as long as $N_{\text{TX,max}}$ is sufficiently high.

Fig. 5. Mutual information per time slot $\mathcal{I}_\text{sys}$ over the number of TXs K for three different MA schemes. Detection thresholds and emitted molecules are chosen optimally subject to different values of the molecule budget $N_{\text{TX,max}}$ per TX per time slot. Differences due to $N_{\text{TX,max}}$ are only visible for NOMA. All other parameters chosen according to Table I. NOMA performs similarly to MDMA even for larger K given sufficiently high $N_{\text{TX,max}}$.

The effects for $N_{\text{TX,max}} = 10^5$ are largely the same as for $N_{\text{TX,max}} = 10^6$, except that even for very high SNR the performance of DBMC-NOMA reaches a constant plateau C with $\mathcal{I}_\text{sys}^\text{NOMA} \approx C < \mathcal{I}_\text{sys}^\text{MDMA}$. In Section IV-A2, we saw the performance not only determined by the optimal ΔN_TX but also by the absolute number of molecules due to the signal-dependent standard deviation of the DBMC signal. For smaller $N_{\text{TX,max}}$, the maximum achievable $\mathcal{I}_\text{sys}^\text{NOMA}$ will therefore decrease and vice-versa.

2) Varying Network Size: In Figure 5, the number of TXs is varied on the x-axis with $\mathcal{I}_\text{sys}$ per time slot on the y-axis. Additionally, the performance of DBMC-NOMA is shown for multiple values of $N_{\text{TX,max}}$. Looking first at TDMA and MDMA, the results show that $\mathcal{I}_\text{sys}^\text{TDMA} = 1$ bit/slot for all network sizes K, while $\mathcal{I}_\text{sys}^\text{MDMA} = K$ bit/slot. TDMA and MDMA are only shown once since their performance is the same for the chosen values of $N_{\text{TX,max}}$. This is the case since increasing K increases the MAI, which is only present for DBMC-NOMA, as shown in (5) and (6).

Again, we see that DBMC-NOMA slots in between TDMA and MDMA as lower and upper bound, respectively. Similar to the results in Figure 4, there are two regimes with a transition between them. In the low-K regime, we observe that $\mathcal{I}_\text{sys}^\text{NOMA} \approx K = \mathcal{I}_\text{sys}^\text{MDMA}$. In the high-$K$ regime, we have $\mathcal{I}_\text{sys}^\text{NOMA} \approx C < \mathcal{I}_\text{sys}^\text{MDMA}$ with the performance reaching a constant plateau C parallel to $\mathcal{I}_\text{sys}^\text{TDMA}$. In this regime, any additional TX is allocated $N_{\text{TX},i} = 0$, when optimizing the number of emitted molecules. This is again due to the optimization goal being a system-wide metric. Crucially, the transition to and level of the plateau C depend on the available molecule budget. If $N_{\text{TX,max}}$ increases, the number of TXs served by DBMC-NOMA with the same performance as MDMA increases. As seen in Section IV-A2, the relative standard deviation around the signal mean decreases with a higher number of emitted molecules. Here, this results in a higher effectiveness of the SIC in separating the signals of
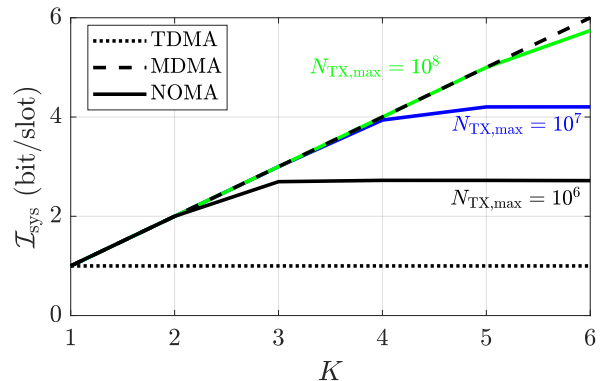
larger numbers of different TXs. This suggests that given a sufficiently high molecule budget, DBMC-NOMA will reach the performance of MDMA for any K. The rigorous confirmation of this point is left for future work.

V. CONCLUSION

In this paper, we proposed using NOMA for a DBMC network with K TXs and a central receiver oriented on an IoBNT use case. The performance of the DBMC-NOMA approach was evaluated and compared to TDMA and MDMA with respect to the mutual information per time slot under various conditions. In particular, we showed that the performance of a DBMC-NOMA system can be optimized based on the emitted number of molecules per TX. We presented an analytical derivation of the BEP of the system using the DBMC-NOMA approach, taking into account both ISI and MAI. The results show that optimizing the emitted number of molecules per TX enables DBMC-NOMA to perform on the same level as MDMA and outperform TDMA using only one molecule type. Additionally, we illustrated the importance of sufficiently high SNR and molecule budget for DBMC-NOMA to achieve the highest possible performance.

This work highlights that DBMC power control methods, i.e. protocols that adjust the emitted number of molecules, should be explored further. Future work on DBMC-NOMA should incorporate fairness measures among TXs. More detailed analysis of the different MA methods for DBMC will be crucial for developing a comprehensive DBMC resource allocation framework.

REFERENCES

[1] I. F. Akyildiz, M. Pierobon, S. Balasubramaniam, and Y. Koucheryavy, "The Internet of Bio-Nano Things," *IEEE Commun. Mag.*, vol. 53, pp. 32–40, Mar. 2015.
[2] E. Shitiri and H.-S. Cho, "A TDMA-Based Data Gathering Protocol for Molecular Communication via Diffusion-Based Nano-Sensor Networks," *IEEE Sensors Journal*, vol. 21, pp. 19582–19595, Sept. 2021.

[3] L. Chouhan and M.-S. Alouini, "Rescaled Brownian Motion of Molecules and Devices in Three-Dimensional Multiuser Mobile Molecular Communication Systems," *IEEE Trans. Wirel. Commun.*, vol. 21, pp. 10472–10488, Dec. 2022.

[4] Y. Saito, Y. Kishiyama, A. Benjebbour, T. Nakamura, A. Li, and K. Higuchi, "Non-Orthogonal Multiple Access (NOMA) for Cellular Future Radio Access," in *2013 IEEE Proc. 77th Veh. Technol. Conf. (VTC Spring)*, (Dresden, Germany), pp. 1–5, June 2013.

[5] B. Krishnaswamy, Y. Jian, C. M. Austin, J. E. Perdomo, S. C. Patel, B. K. Hammer, C. R. Forest, and R. Sivakumar, "ADMA: Amplitude-Division Multiple Access for Bacterial Communication Networks," *IEEE Trans. Mol. Biol. Multi-Scale Commun.*, vol. 3, pp. 134–149, Sept. 2017.

[6] A. Wietfeld, S. Schmidt, and W. Kellerer, "Non-Orthogonal Multiple Access for Diffusion-Based Molecular Communication Networks," in *Proc. 10th ACM Int. Conf. Nanoscale Comput. Commun.*, (Coventry, UK), pp. 1–2, Sept. 2023. work-in-progress paper, presented as a poster.

[7] V. Jamali, A. Ahmadzadeh, W. Wicke, A. Noel, and R. Schober, "Channel Modeling for Diffusive Molecular Communication—A Tutorial Review," *Proc. IEEE*, vol. 107, pp. 1256–1301, July 2019.

[8] H. K. Rudsari, N. Mokari, M. R. Javan, E. A. Jorswieck, and M. Orooji, "Drug Release Management for Dynamic TDMA-Based Molecular Communication," *Trans. Mol. Biol. Multi-Scale Commun.*, vol. 5, pp. 233–246, Dec. 2019.

[9] L. Shi and L.-L. Yang, "Error Performance Analysis of Diffusive Molecular Communication Systems With On-Off Keying Modulation," *IEEE Trans. Mol. Biol. Multi-Scale Commun.*, vol. 3, pp. 224–238, Dec. 2017.

[10] T. M. Cover and J. A. Thomas, *Elements of Information Theory*. Wiley Series in Telecommunications, New York: Wiley, 1991.

APPENDIX

To calculate the probability of occurrence of the previous $j-1$ decoded symbols, $\underline{\hat{s}}_{j-1}$, we first note that it can be written as the following multiplication of conditional probabilities of a single decoded symbol

$$\mathbb{P}(\underline{\hat{s}}_{j-1} = \underline{\hat{s}}'_{j-1} | \mathbf{S} = \mathbf{S}', s_j[0] = x)$$
$$= \prod_{i=1}^{j-1} \mathbb{P}\left(\hat{s}_i = \hat{s}'_i | \mathbf{S} = \mathbf{S}', s_j[0] = x, \underline{\hat{s}}_{i-1} = \underline{\hat{s}}'_{i-1}\right). \quad (17)$$

To now calculate the individual factors, we first define

$$P_{\text{prev}}\left(i, \mathbf{S}, \underline{\hat{s}}_{i-1}\right) =$$
$$\mathcal{P}_{\text{CDF}}\left(\tau_i - 1 + \sum_{m=1}^{i-1} \hat{s}_m \lambda_{m,i,0}; \mathbf{S} \cdot \Lambda_i + \lambda_{\text{n}}\right). \quad (18)$$

The probability of a decoded symbol is then expressed for the four different possible cases as follows

$$\mathbb{P}\left(\hat{s}_i = \hat{s}'_i | \mathbf{S} = \mathbf{S}', s_j[0] = x, \underline{\hat{s}}_{i-1} = \underline{\hat{s}}'_{i-1}\right)$$
$$= \begin{cases} 1 - P_{\text{prev}}\left(i, \mathbf{S}, \underline{\hat{s}}_{i-1}\right) & s_{i,0} = \hat{s}_i \text{ AND } s_{i,0} = 0 \\ 1 - P_{\text{prev}}\left(i, \mathbf{S}, \underline{\hat{s}}_{i-1}\right) & s_{i,0} \neq \hat{s}_i \text{ AND } s_{i,0} = 1 \\ P_{\text{prev}}\left(i, \mathbf{S}, \underline{\hat{s}}_{i-1}\right) & s_{i,0} = \hat{s}_i \text{ AND } s_{i,0} = 1 \\ P_{\text{prev}}\left(i, \mathbf{S}, \underline{\hat{s}}_{i-1}\right) & s_{i,0} \neq \hat{s}_i \text{ AND } s_{i,0} = 0 \end{cases}. \quad (19)$$

Inserting (18) into (19), and (19) into (17) yields the desired probability.